FORECASTERS' FORUM

A Comparison of Right-Moving Supercell and Quasi-Linear Convective System Tornadoes in the Contiguous United States 2003–21

RICHARD L. THOMPSON[a]

[a] *NOAA/NWS/NCEP/Storm Prediction Center, Norman, Oklahoma*

(Manuscript received 14 January 2023, in final form 13 May 2023, accepted 16 May 2023)

ABSTRACT: Tornadoes produced by right-moving supercells (RMs) and quasi-linear convective systems (QLCSs) are compared across the contiguous United States for the period 2003–21, based on the maximum F/EF-scale rating per hour on a 40-km horizontal grid. The frequency of QLCS tornadoes has increased dramatically since 2003, while the frequency of RM tornadoes has decreased during that same period. The finding of prior work that the most common damage rating for QLCS tornadoes at night is EF1 persists in this larger, independent sample. A comparison of WSR-88D radar attributes between RM and QLCS tornadoes shows no appreciable differences between EF0 tornadoes produced by either convective mode. Differences become apparent for EF1–2 tornadoes, where rotational velocity is larger and velocity couplet diameter is smaller for RM tornadoes compared to QLCS tornadoes. The frequency of tornadic debris signatures (TDSs) in dual-polarization data is also larger for EF1–2 RM tornadoes when controlling for tornadoes sampled relatively close to the radar sites and in those occurring during daylight versus overnight. The weaker rotational velocities, broader velocity couplet diameters, and lower frequencies of TDSs both close to the radar and at night for QLCS EF1 tornadoes suggest that a combination of inadequate radar sampling and occasional misclassification of wind damage may be responsible for the irregularities in the historical record of QLCS tornado reports.

SIGNIFICANCE STATEMENT: A comparison of radar attributes between tornadoes with right-moving supercells and squall-line mesovortices suggests some irregularities in squall-line tornado records in the contiguous United States. The irregularities appear to be the result of both inadequate radar sampling for the relatively shallow squall-line tornadoes and occasional misclassification of wind damage with the lack of other corroborating evidence, especially overnight.

KEYWORDS: Forecasting techniques; Nowcasting; Operational forecasting; Tornadoes

1. Introduction

The threat to life and property increases dramatically as tornado intensity increases, such that the vast majority of tornado fatalities are the result of significant (F/EF2+ rated damage) tornadoes, which account for less than 15% of all tornado reports (Ashley 2007; Anderson-Frey and Brooks 2019). The majority of these significant tornadoes in the United States are produced by right-moving supercells (RMs) (Smith et al. 2012; Brotzge et al. 2013), and RMs have garnered the majority of the attention of the research, forecasting, and emergency management communities during the past several decades (e.g., Brooks et al. 2019).

Approximately 21% of all tornadoes in the United States are produced by quasi-linear convective systems (QLCSs; Ashley et al. 2019), in general agreement with the previous findings of Trapp et al. (2005) and Smith et al. (2012); however, each of these studies varied in exactly what was considered a QLCS tornado [i.e., Ashley et al. (2019) and Trapp et al. (2005) likely included supercells embedded in a QLCS, whereas Smith et al. (2012) did not]. QLCS tornadoes tend to produce primarily weak (F/EF0–1) damage (Trapp et al. 2005; Gallus et al. 2008; Smith et al. 2012), and QLCS tornado reports have increased over time (Ashley et al. 2019). Examples of RM and QLCS EF1 tornadic storms are shown in Fig. 1.

Trapp and Weisman (2003) and Weisman and Trapp (2003) examined mesovortex formation in QLCSs from a theoretical perspective, focusing on a balance between low-level, vertical wind shear in the ambient environment and vertical circulations generated by the QLCS cold pool. Additional work by Atkins and St. Laurent (2009a,b) identified two potential mechanisms responsible for mesovortex formation in QLCSs:

1) A cyclonic-only mesovortex forms as horizontal baroclinic vorticity (parallel to gust front) is tilted downward to become cyclonic on the equatorward (Northern Hemisphere) side of a downdraft, which combines with streamwise vorticity in the storm inflow to support mesovortex formation.
2) A cyclonic–anticyclonic vortex couplet (cyclonic poleward, anticyclonic equatorward in the Northern Hemisphere) results from a rear-inflow jet/downdraft surge that enhances the low-level updraft on the nose of the surge/bow echo, and this updraft tilts barolinic vorticity generated along the gust front, in addition to streamwise vorticity from storm inflow.

Corresponding author: Richard L. Thompson, richard.thompson@noaa.gov

DOI: 10.1175/WAF-D-23-0006.1

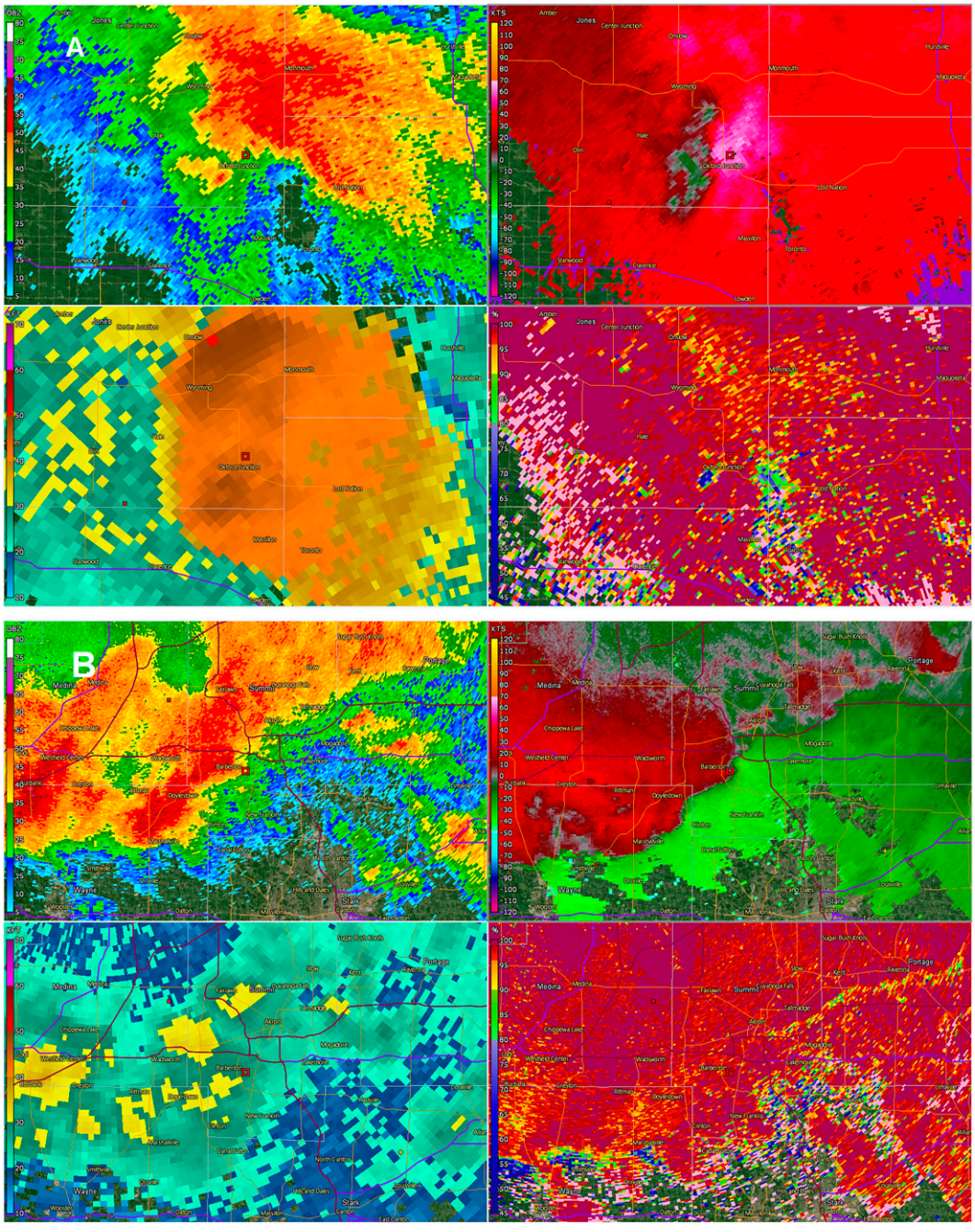

FIG. 1. Four-panel WSR-88D displays with EF1 tornadoes produced by (a) an RM at 0058 UTC 29 Jun 2017 [Davenport, IA (KDVN), site to the lower right] and b) a QLCS at 0355 UTC 8 Apr 2020 [Cleveland, OH (KCLE), site to the upper left]. The top-left, top-right, and bottom-right panels in each group are the 0.5° scan of base reflectivity (dBZ), storm-relative velocity (kt), and cross-polar correlation coefficient, respectively. The bottom-left panel is the estimated echo tops (thousands of feet).

Parker et al. (2020) identified additional complexity through their documentation of multiple modes of mesovortex formation within a single QLCS—a mix of the aforementioned baroclinic/cold-pool processes and a more supercell-like process whereby tilting of horizontal vorticity (vortex lines orthogonal to the gust front) by updrafts supports mesovortex formation (Flournoy and Coniglio 2019). Relatively little work has focused on the thermodynamic characteristics of QLCS cold pools with respect to tornado production. McDonald and Weiss (2021) examined a small sample of southeast U.S. RMs and QLCSs and found only small

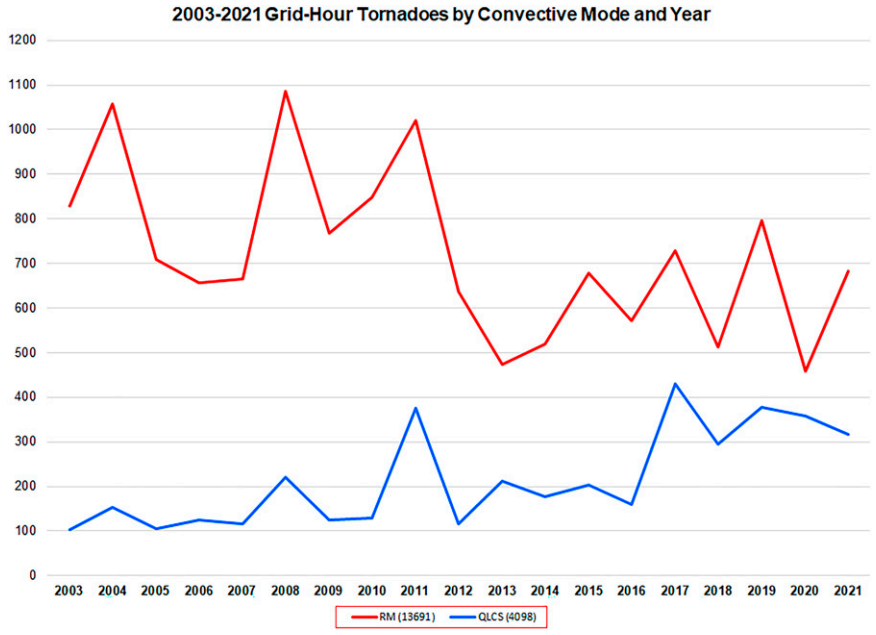

FIG. 2. Counts of RM and QLCS tornadoes (*y* axis) by year (*x* axis) on a 40-km horizontal grid per hour across the CONUS, for the period 2003–21.

differences in the cold-pool potential temperature deficits between nontornadic and weakly tornadic events.

No clear consensus has yet emerged regarding the dominant mechanism for mesovortex formation (assuming a single mechanism is most common), whether it is downward tilting of crosswise vorticity along the gust front, baroclinic vorticity generation within the cold pool (Schenkman and Xue 2016), or upward tilting of streamwise vorticity within the storm inflow region. This lack of a clear consensus for QLCS tornado formation may contribute to the inability to consistently and accurately anticipate QLCS tornado formation, which is reflected in lower probability of detection (Anderson-Frey et al. 2016) and shorter lead times (~4 min less; Brotzge et al. 2013) for QLCS tornado warnings. Warning performance is

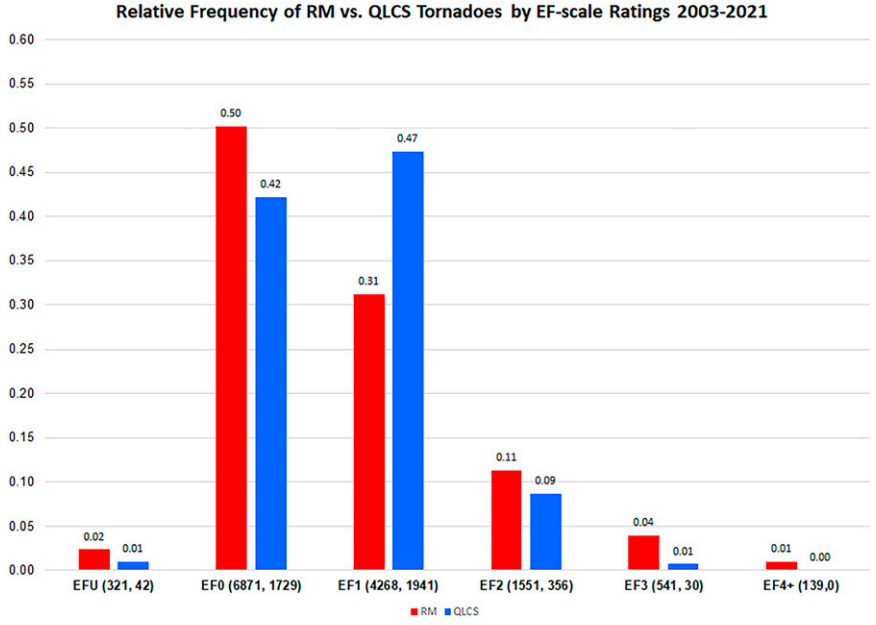

FIG. 3. Relative frequencies of RM and QLCS tornadoes by F/EF-scale rating category, with sample sizes in parentheses (RM on the left, QLCS on the right).

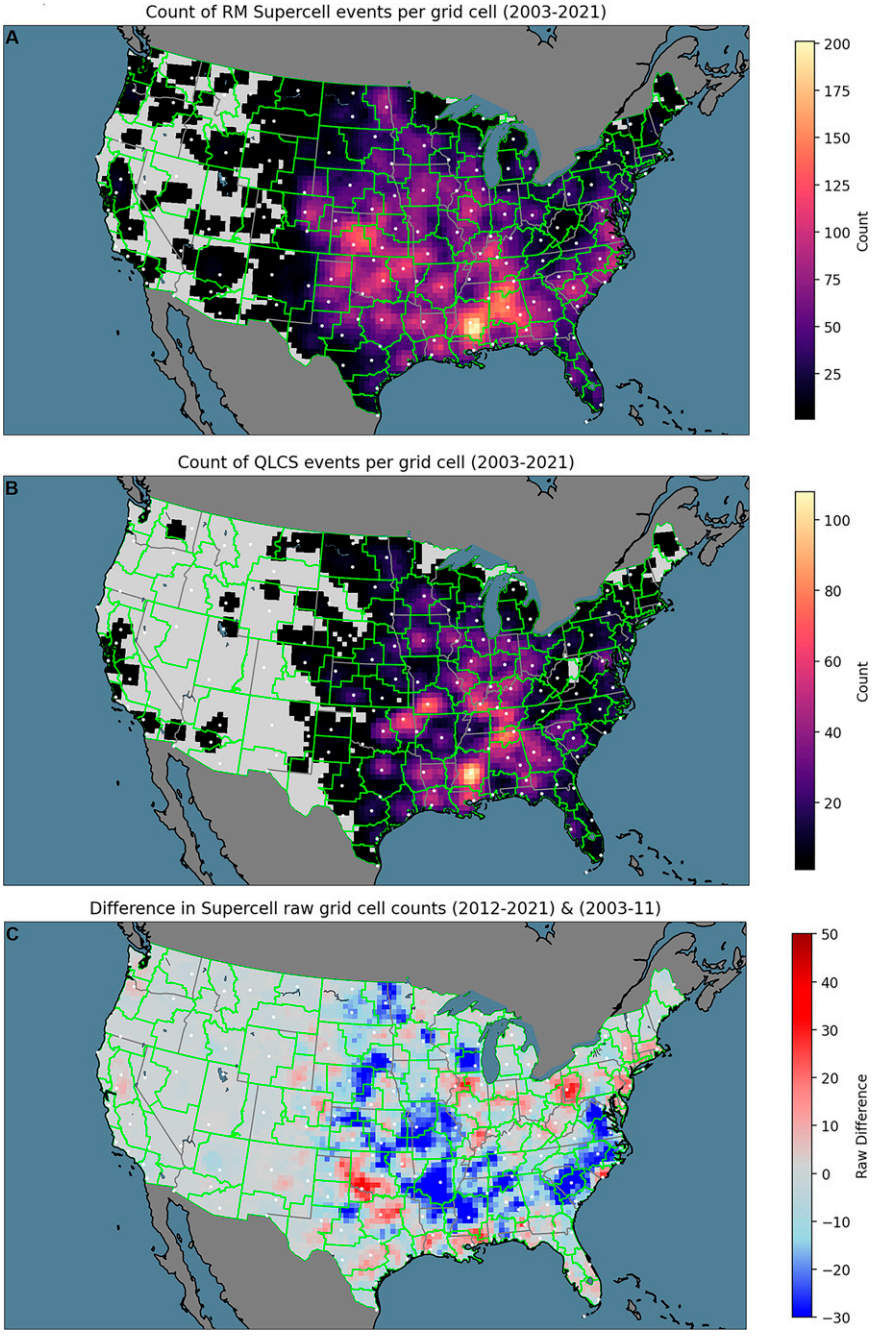

FIG. 4. Raw grid-hour tornado counts for 2003–21 (a) RM and (b) QLCS. Raw grid-hour changes from 2003–11 to 2012–21 for (c) RM and (d) QLCS. Percent changes in tornado reports are shown in (e) RM and (f) QLCS, masked for a minimum of 20 total events per grid in the full 2003–21 period. Data are plotted on the 40-km horizontal grid matching Smith et al. (2012), and boundaries of NWS county warning areas are displayed in light green.

also likely hindered by the relatively short-lived and shallow nature of QLCS tornadoes compared to RM tornadoes.

Regardless of the explicit mechanisms driving QLCS tornado formation, part of the increase in QLCS tornado reports, as discussed by Ashley et al. (2019), can be attributed to an emphasis on short-term forecasting techniques like the three-ingredients method outlined by Schaumann and Przybylinksi (2012). The three-ingredients method focuses on anticipation of mesovortex formation in bowing segments of a QLCS where the inflow–outflow interface (gust front denoted by a wind shift in radar velocity data) is vertically aligned with the updrafts (denoted by the high-reflectivity band along the

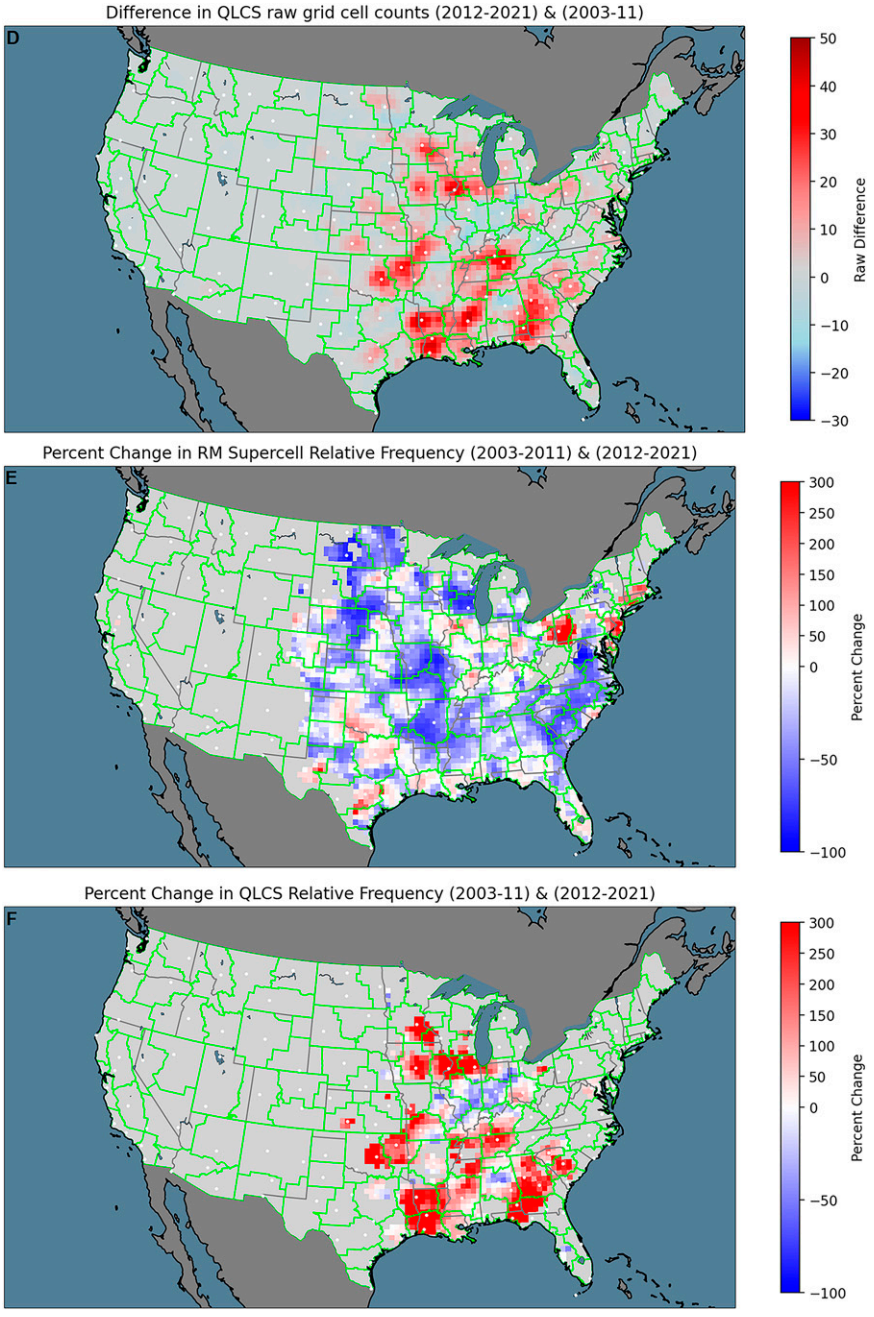

FIG. 4. (*Continued*)

QLCS in radar reflectivity). Mesovortex formation is expected along the bowing QLCS segments where the component of the 0–3-km bulk shear vector orthogonal to the line exceeds 30 kt (15 m s^{-1}), representing areas of potential balance between the cold pool and low-level vertical wind shear. Given the primarily radar-centric nature of the three-ingredients method, improvements in radar sampling, such as the introduction of superresolution velocity data (Brown et al. 2005; Torres and Curtis 2007), dual polarization data [i.e., tornadic debris signature (TDS) detection], and more rapid updates to low-level scans (Chrisman 2014) have all led to increased detection of QLCS mesovortices and associated tornadoes.

Trapp et al. (2005) speculated an underreporting of QLCS tornadoes of up to 12% based on a disproportionate number of tornado damage ratings of F1 in their 3-yr sample of QLCS tornadoes from 1999 to 2001. Large numbers of tornadoes have been identified in individual warm-season case studies of events like those of 31 August 2014 across Iowa (Skow and Cogil 2017) and 30 June 2014 across northwestern Indiana (Lyza et al. 2019). Detailed ground surveys, postevent aerial

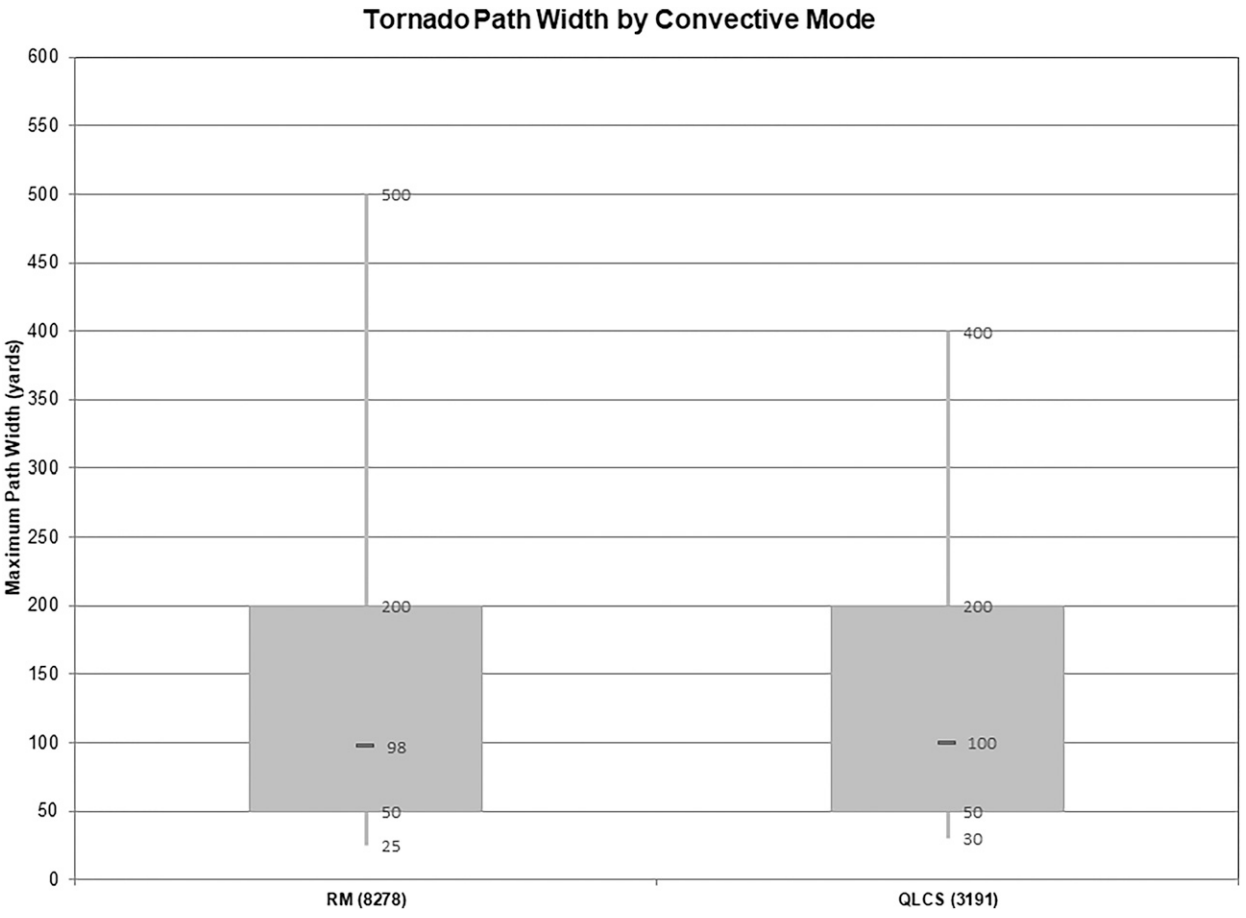

FIG. 5. Box-and-whiskers plot of maximum tornado damage-path widths (yards) for RM and QLCS tornadoes across the contiguous United States for the full 2003–21 grid-hour tornado sample. The boxes display the 25th–75th percentiles (including the median), and the whiskers extend to the 90th and 10th percentiles.

imagery, and analysis of WSR-88D data were part of each case study, and they provided recommendations for TDS (Ryzhkov et al. 2005; Schultz et al. 2012a,b; Van Den Broeke and Jauernic 2014) identification and potential warning strategies for QLCS tornadoes. Many QLCS tornadoes have been reported in other events since 2016 during the spring across the eastern Great Plains, the summer across the Midwest, and during the cool season across the Southeast (e.g., the convective mode sample documented in Lyons et al. 2022).

The increase in QLCS tornado reports is not without question, however. Few QLCS tornadoes are accompanied by clear, visual evidence of a condensation funnel compared to RM tornadoes that tend to last longer and/or occur in more open areas of the Great Plains. QLCS tornado reports are also more prevalent at night compared to RM tornadoes (Trapp et al. 2005; Ashley et al. 2019). Thus, the majority of QLCS tornadoes are based primarily on damage reports, with a documented tendency for a greater relative frequency of F/EF1 maximum damage reports (Trapp et al. 2005) compared to RM tornadoes. Given the occasional ambiguity in discriminating F/EF0–1 tornado damage, characterized by convergent damage patterns, from other so-called straight-line wind damage with either unidirectional or divergent patterns in damage, there are reasons to question the veracity of some QLCS tornado reports, as discussed by Ashley at al. (2019).

Obviously, there are near-storm environments that are more favorable for stronger tornadoes with both RMs and QLCSs (e.g., Thompson et al. 2012). Likewise, there are stronger WSR-88D signatures [i.e., low-level rotational velocity $>$ 30–40 kt ($\sim$15–20 m s^{-1}; hereafter, V_{rot}), per Thompson et al. 2017, hereafter T17] that more clearly correspond to higher probabilities of any tornado and are correlated with the potential strength of a tornado. This work focuses on two primary questions:

1) Are WSR-88D signatures associated with QLCS and RM tornadoes different?
2) Do the differences in radar signatures corroborate differences in reporting tendencies between QLCS and RM tornadoes?

2. Data and methods

To answer the questions posed in the introduction, case selection followed the grid-hour filtering procedure outlined in

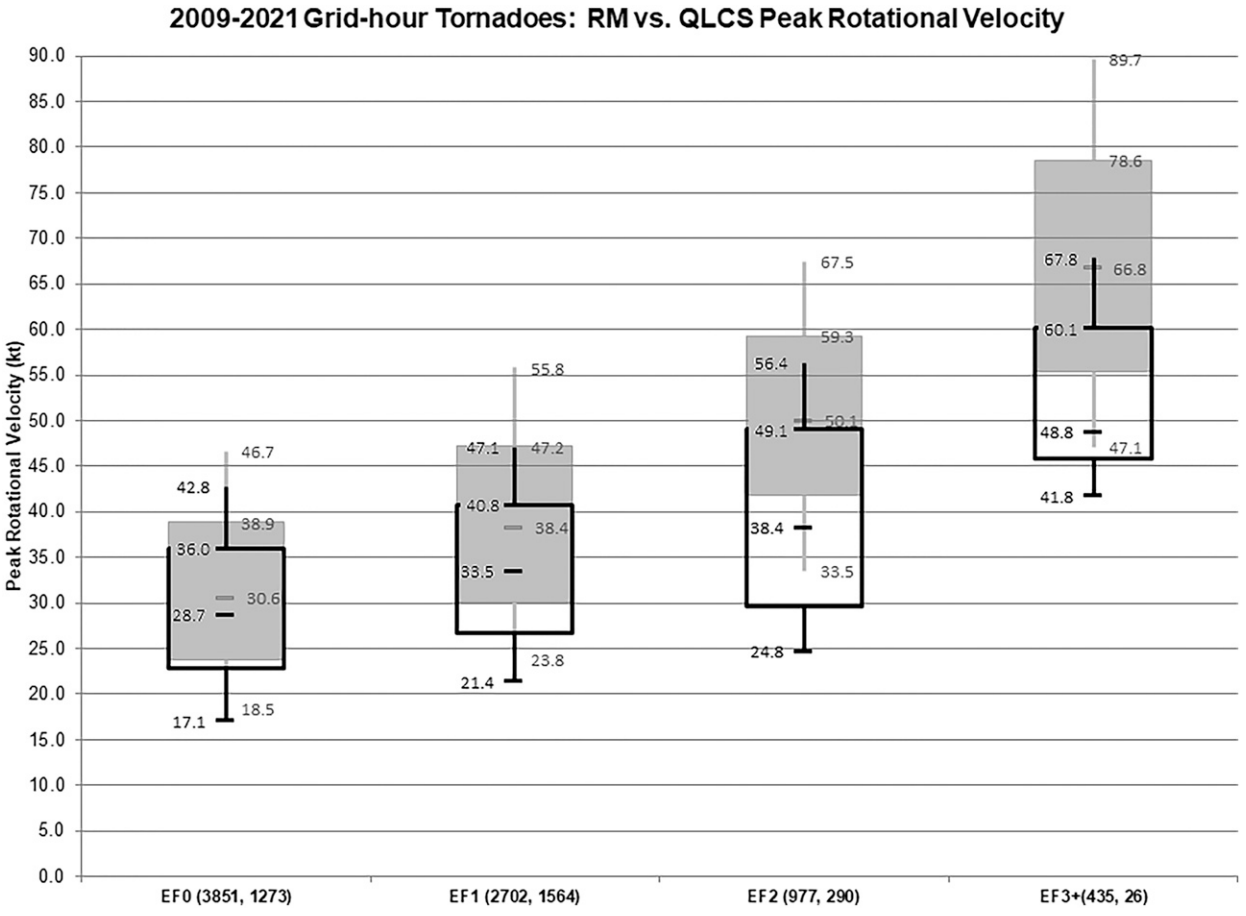

FIG. 6. As in Fig. 5, but for peak V_{rot} by maximum EF-scale damage ratings, for RM (solid gray) and QLCS (black outline) grid-hour tornadoes from 2009 to 2021.

Smith et al. (2012), where the maximum tornado F/EF-scale damage rating is retained per hour on a 40-km horizontal grid that matches the Storm Prediction Center hourly mesoanalysis system (Bothwell et al. 2002). Convective mode was assigned to each grid-hour tornado event, based on a manual interpretation of full volumetric level II WSR-88D data in the scan immediately preceding the start of each grid-hour tornado via Gibson Ridge Level II radar-viewing software (http://www.grlevelx.com/), as in Smith et al. (2012). Only RM (discrete, cluster, and cell in line) and QLCS tornadoes (mutually exclusive) are considered in this work.

The grid-hour filtering procedure retained ~80% of the total number of tornadoes within each grid during each hour (Smith et al. 2012). Once the first occurrence of the maximum F/EF-scale damage rating was determined, all additional tornadoes were filtered out from the grid box during each hour. In effect, the grid-hour filtering focused on the most intense tornadoes at the expense of clustering of weaker tornadoes within the same grid hour. Once the convective mode was identified for each grid-hour event, the peak cyclonic V_{rot} (defined as the average of the magnitudes of the maximum inbound and outbound velocity gates, as in Smith et al. 2015 and T17) was manually extracted. T17 created a 2-yr "null" sample of V_{rot} associated with nontornadic severe thunderstorms, as well as corresponding convective modes. The T17 findings are applicable to this work in that they allow tornado probability estimates for each reported tornado, based on binned ranges of couplet diameter (the linear distance between the centroids of the maximum inbound and outbound velocity gates), the height above radar level (ARL; whereby lower heights correspond to closer to the radar site), and V_{rot} values for an independent sample. Observed maximum tornado-path widths for each grid-hour event were retained for comparison with the WSR-88D attributes.

TDSs were identified and examined for a subset of EF1 tornadoes when the following criteria were met: at least one range gate with a minimum cross-polar correlation coefficient (CC) $< 92\%$, coincident with both a primarily cyclonic velocity couplet and reflectivity > 20 dBZ. TDS height relied on contiguous TDS criteria in successively higher-elevation scans (sloping with height in the direction of tornado movement) until one or more of the criteria were no longer satisfied (typically CC rose above 92% or there was no longer an identifiable, cyclonic velocity couplet). In the case of noisy CC data, such as nonuniform beam filling, TDS identification was not always possible.

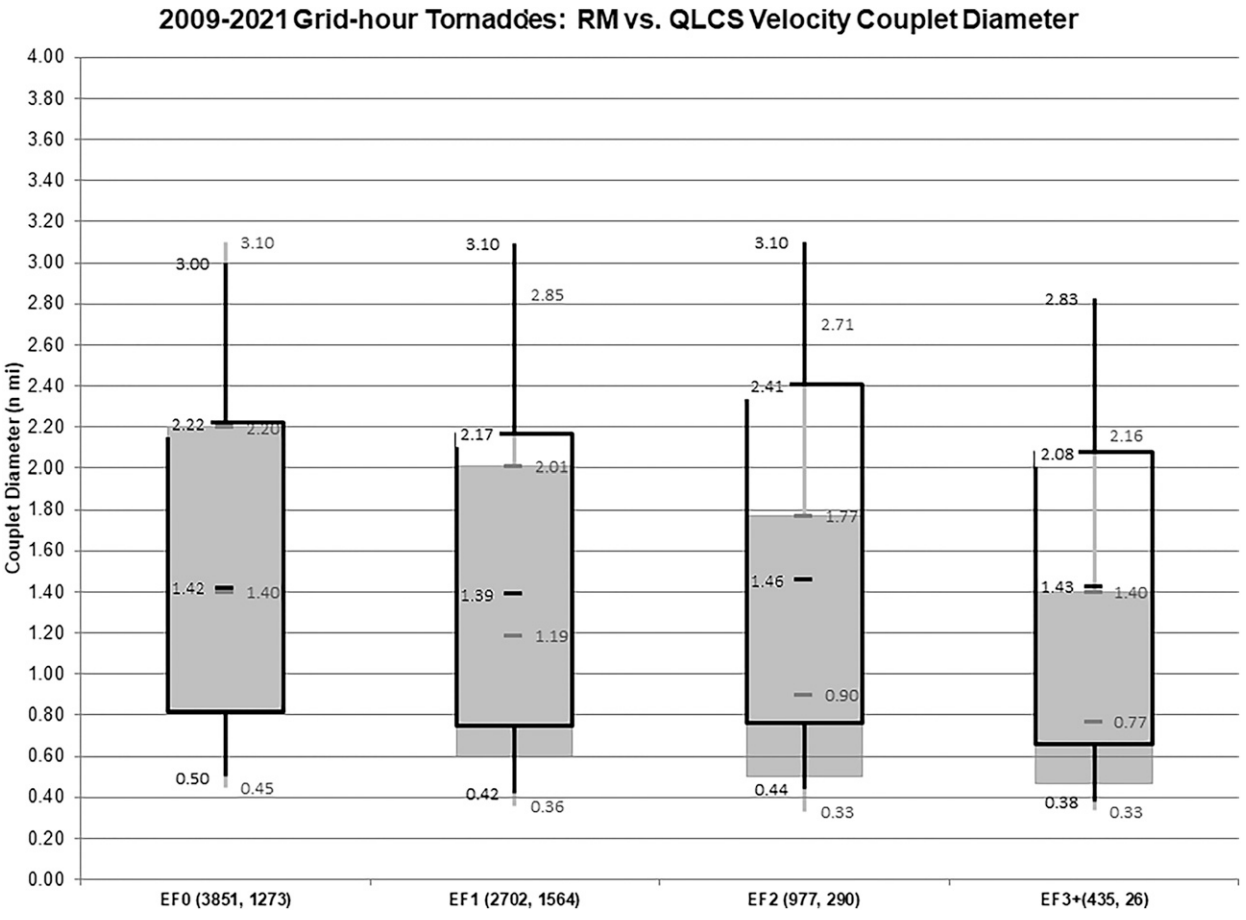

FIG. 7. As in Fig. 6, but for velocity couplet diameter (n mi) at the time of peak V_{rot}.

3. Results

The number of QLCS tornadoes has increased since 2003 and the greatest numbers of summer, fall, and winter QLCS grid-hour tornadoes have all occurred since 2017 (Fig. 2). Conversely, the number of RM tornadoes has generally decreased since the very active spring of 2011. Neither the convective-mode classification scheme nor the key contributors to the convective-mode database have changed since the report of Smith et al. (2012), so changes in this database over time are unlikely to be the result of changes in storm classification. An eastward shift in environments favoring RM tornadoes from the Great Plains toward the Mississippi Valley was documented by Gensini and Brooks (2018), and additional work is justified to explore the environmental aspects of the changes in the grid-hour tornado reports from 2003 to 2021.

Similar to Trapp et al. (2005), who considered tornadoes from 1999 to 2001, an unusually large relative frequency of F/EF1 QLCS tornadoes (Fig. 3) persists in this sample from 2003 to 2021, with 47% of QLCS tornadoes rated F/EF1 and only 42% of QLCS tornadoes rated F/EF0. Edwards et al. (2021) noted a clear increase in the overall frequency of EF1 tornadoes with implementation of the EF scale in 2007. With such obvious changes in tornado reporting by convective mode, exemplified in Fig. 2, the spatial distribution of these changes should be explored. The full sample of tornadoes was separated into two temporal periods: 1) 2003–11 matching Smith et al. (2012), and 2) 2012–21. These two periods correspond well with the observed changes in RM and QLCS tornado frequency, as illustrated spatially in Fig. 4. RM tornadoes are most common for the full 2003–21 period from Mississippi and Alabama to Kansas and Oklahoma (Fig. 4a), while QLCS tornadoes are most common from the lower Mississippi Valley into the Ohio Valley (Fig. 4b). Some tendency for report clustering near radar sites is noted with both RM and QLCS tornadoes. One obvious feature in Fig. 4c is the broad area of decreases in RM tornadoes across the traditional areas of greatest RM tornado frequency from the first period to the more recent period (Kansas and Nebraska to Mississippi and Alabama and the Carolinas), though the changes are lower in terms of percentage decreases (Fig. 4e). The larger percentage increases noted across eastern Ohio are in an area where RM tornadoes are relatively less common, such that smaller numerical increases result in larger percentage increases. Pronounced increases in the numbers of QLCS tornado reports have occurred (Fig. 4d), with large local increases tending to focus relatively closer to radar sites (white dots in Fig. 4d). There are some indications of

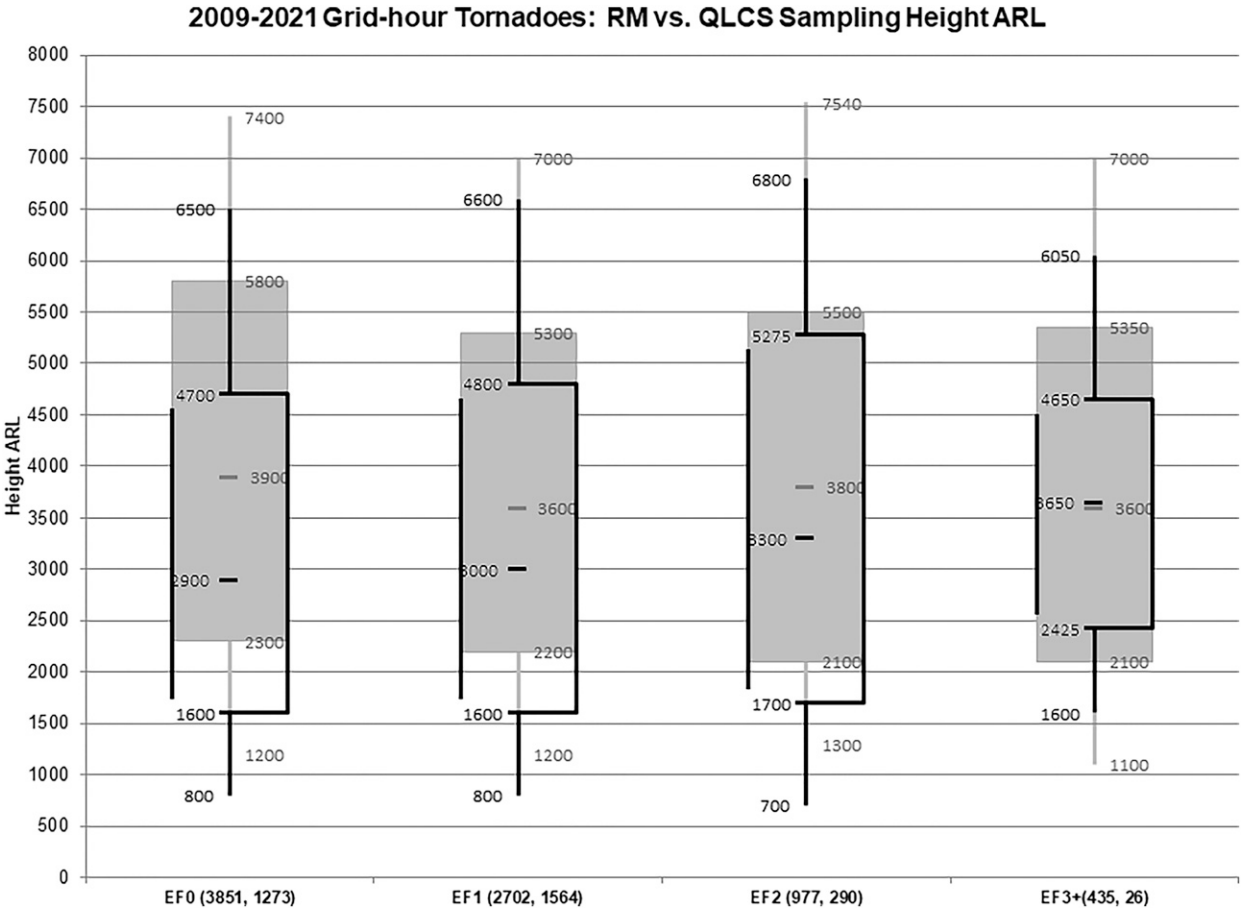

FIG. 8. As in Fig. 6, but for height ARL of the highest velocity gate with each peak V_{rot}.

reporting changes aligning with National Weather Service (NWS) county warning area borders (green outlines in Fig. 4), primarily across parts of the lower Mississippi Valley and the Southeast. However, net changes in QLCS tornado reports have been smaller across the traditional area of greatest QLCS tornado occurrence (i.e., the Ohio Valley; Trapp et al. 2005; Smith et al. 2012; Lyons et al. 2022). The reasons for the smaller changes in the traditional QLCS tornado belt are not known with high confidence, though earlier application of the three-ingredients method (prior to 2012) at the local NWS office level could explain the more muted changes in QLCS tornadoes from the first period to the second period (beginning in 2012).

Before considering radar signatures associated with the RM and QLCS tornadoes in this sample, the ability of the WSR-88D to resolve tornado-related signatures must be considered. A logical approach is to compare maximum tornado-path widths, which should scale with tornado-related radar signatures. Observed maximum damage path widths for RM and QLCS tornadoes (Fig. 5) are nearly identical from the 10th through 75th percentile values (RM tornadoes are wider at and above the 90th percentile), so differences in WSR-88D signatures do not appear to be the result of an inability to resolve QLCS tornado-related velocity signatures more so than RM tornadoes (Fig. 5). During the period of this investigation, as mentioned in the introduction, there have been multiple improvements to the WSR-88D that have likely contributed to increases in tornado detection with QLCSs, namely the system-wide introduction of superresolution velocity data by 2007, dual polarization data and the potential for lofted debris detection (TDSs) by 2012, and more rapid base-elevation scan updates since 2014.

Peak V_{rot}, and associated radar attributes at the time of the peak V_{rot} reveal some differences between the radar-sampled velocity couplets associated with RM and QLCS tornadoes. In terms of peak V_{rot}, both RM and QLCS EF0 tornadoes are quite similar, but V_{rot} tends to increase more rapidly with RM tornadoes as EF-ratings increase to EF1 and EF2/EF3 (Fig. 6), which is similar to the findings of Smith et al. (2015; their Fig. 5). The tendency is reversed for velocity couplet diameter, with couplet diameters tending to decrease for more intense RM tornadoes and remaining broader for QLCS tornadoes with the same categorical damage ratings (EF1–3; Fig. 7). The reported QLCS tornado events tend to occur slightly closer to the radar site (a lower height ARL, as shown in Fig. 8), which suggests that the differences are not solely a function of poor radar sampling.

		ARL	ARL	ARL
	Vrot	100–	3000–	6000–
		2900	5900	9900
<1 n mi	10–19.9	**0.25**	**0.25**	0.08
	20–29.9	**0.42**	**0.27**	**0.15**
	30–39.9	**0.63**	**0.47**	**0.41**
	40–49.9	**0.78**	**0.62**	**0.71**
	50–59.9	**0.90**	**0.91**	0.71
	60+	**0.95**	**0.97**	
1–1.99				
n mi	10–19.9	**0.12**	**0.12**	**0.18**
	20–29.9	**0.17**	**0.16**	**0.16**
	30–39.9	**0.32**	**0.27**	**0.19**
	40–49.9	**0.51**	**0.49**	**0.46**
	50–59.9	0.73	**0.67**	0.61
	60+	1.00	0.88	
2–5 n mi	10–19.9	**0.02**	**0.09**	**0.07**
	20–29.9	**0.12**	**0.08**	**0.10**
	30–39.9	**0.10**	**0.18**	**0.14**
	40–49.9	**0.22**	**0.25**	**0.17**
	50–59.9	**0.27**	**0.33**	**0.32**
	60+		0.92	

FIG. 9. Tornado relative frequencies derived from the 2014–15 sample of RM and QLCS grid-hour events from T17, based largely on their Figs. 8–10. The data are grouped into three bins of velocity couplet diameter (n mi), with each subgroup displayed in three ranges of height ARL (columns; ft) and six ranges of peak rotational velocity (V_{rot}; kt). Bold black values denote sample sizes of ≥25 events, gray values denote sample sizes of 10–24 events, and sample sizes of <10 events were left blank. Color shading highlights relative frequency 0.25–0.49 (light peach) and ≥0.50 (dark peach).

While this analysis is limited to reported tornadoes, tornado occurrence is not always known in real time with complete confidence. Thus, it can be useful to consider estimates of tornado relative frequencies that account for false alarms that are inevitable in operational tornado warning situations. Applying the prior work by T17, the relative frequency of tornado occurrence can be estimated from the aforementioned WSR-88D attributes of V_{rot}, couplet diameter and the height ARL for the highest (farthest away) of the two V_{rot} velocity gates. Summarizing T17, tornado relative frequencies increased for larger V_{rot} with smaller couplet diameter, sampled closer to the ground (closer to the radar site). Tornado relative frequencies, based on the three aforementioned radar attributes from a robust sample of severe storms (both QLCS and RM) in 2014–15 by T17, are shown in Fig. 9. The values in Fig. 9 are the raw, binned relative frequencies from Figs. 9 and 10 in T17 with no smoothing or interpolation, plus similar raw values for other combinations not shown explicitly in that paper. Specifically, cases were sorted into three bins by circulation diameter [<1, 1–1.99, and 2–5 n mi (1 n mi = 1.852 km)] and height ARL (100–2900, 3000–5900, and 6000–9900 ft), and the tornado relative frequencies were calculated for six bins of peak V_{rot} (10–19.9, 20–29.9, 30–39.9, 40–49.9, 50–59.9, and ≥60 kt; 1 kt ≈ 0.51 m s^{-1}), which resulted in 54 unique values (four are not displayed due to a sample size of <10 events).

Each of the QLCS and RM grid-hour tornado events was assigned a single tornado relative frequency value from Fig. 9, and the distributions of these values for the independent sample of 2009–21 tornadoes (not including the 2014–15 cases used in T17) are shown in Fig. 10. As in Figs. 6–8, the QLCS and RM samples appear to be quite similar in terms of expected tornado occurrence for EF0 tornadoes in the range of V_{rot} where both sample sizes are relatively large (i.e., <50 kt; per Fig. 9 in T17). Differences become more pronounced for EF2+ tornadoes, with consistently higher relative frequencies based on WSR-88D signatures for RMs versus QLCSs. The higher tornado relative frequencies with RM tornadoes (i.e., the roughly one quartile offset of the interquartile ranges) reflect the influence of the tighter velocity couplets from Fig. 7, while the radar attributes (and resultant tornado relative frequencies) change much less as tornado damage ratings increase from EF0 to EF2+ with QLCS tornadoes. Only 38% of the RM EF2+ tornadoes from 2009 to 2021 were associated with peak V_{rot} < 50 kt, while 76% of the QLCS EF2+ tornadoes were associated with peak V_{rot} below this threshold. The net result is that discrimination between strong (EF2+) and weak (EF0–1) QLCS tornadoes is more difficult compared to RM tornadoes, which agrees with the findings of T17 (see their Figs. 8–10). Tornado relative frequency distributions are nearly identical for RM and QLCS EF0 tornadoes, and ~93%–96% of EF0 tornadoes with each convective mode are associated with peak V_{rot} < 50 kt.

4. Discussion

The percentage of TDSs by maximum EF rating (Fig. 11) supports the possibility of some reporting irregularities with QLCS compared to RM tornadoes. For example, a TDS was evident for a larger percentage of QLCS EF0 tornadoes than RM tornadoes, even though the other radar attributes were essentially indistinguishable (i.e., Figs. 6–8). This could be related to an underreporting of weak QLCS tornadoes [as speculated by Trapp et al. (2005)], though it is plausible that the difference is also largely the result of RM EF0 tornadoes that are observed more frequently in open areas of the Great Plains with few potential damage indicators. When considering only cases observed relatively close to the radar (<3000 ft ARL), QLCS EF0 tornadoes are associated with a TDS more frequently than are RM EF0 tornadoes [40% vs. 33%, respectively (not

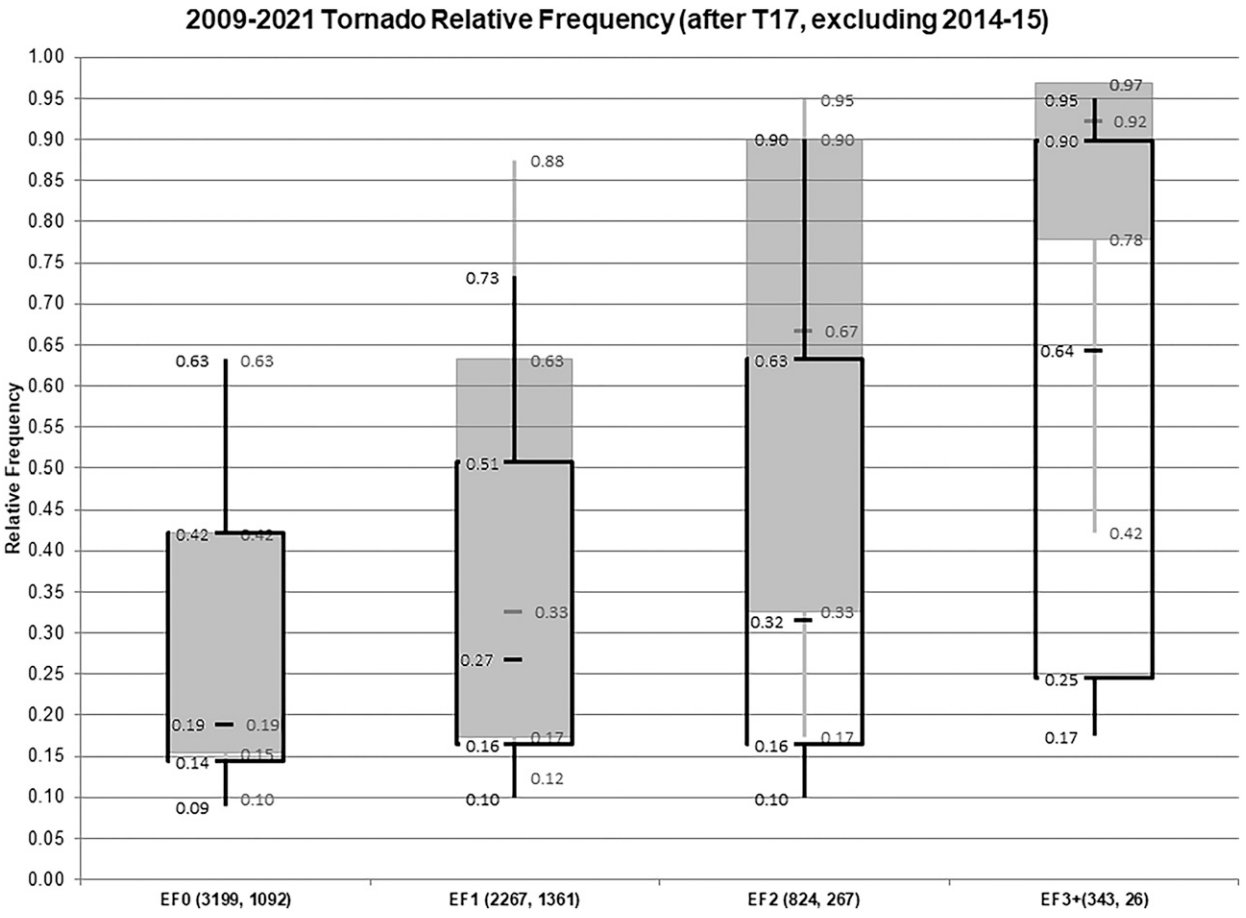

FIG. 10. As in Fig. 6, but for tornado relative frequencies based on peak V_{rot}, velocity couplet diameter, and sampling height ARL. This plot estimates the relative frequency of tornado occurrence (in the absence of a TDS or spotter reports confirming a tornado), and the values were derived from the independent sample presented in T17.

shown)]. Continuing with events close to the radar sites, RM EF1 tornadoes produced a TDS almost two-thirds of the time (~64%), while QLCS EF1 tornadoes produced a TDS roughly half of the time (51%; Table 1). The tendency for QLCS tornadoes to occur more frequently to the east of the Great Plains (the mean longitude of all QLCS tornadoes in this sample with dual-polarization data available is 89.20°W, and the same for RM tornadoes, 90.22°W), where potential damage indicators and population density are generally greater, is at odds with the lower relative frequency of TDSs compared to RM tornadoes in the range of EF1–2 peak damage ratings.

Some of the difference in TDS relative frequency is related to WSR-88D sampling in QLCS tornado events. Maximum TDS heights are lower with EF1 QLCS tornadoes (Fig. 12), and the relative frequency of TDSs increases as sampling occurs closer to the radar site (lower heights ARL; Table 1), though RM EF1 tornadoes still produce a higher relative frequency of TDSs. RMs clearly tend to produce deeper TDSs for the same (EF1) peak damage ratings, which indirectly suggests the presence of stronger and deeper updrafts associated with RM tornadoes. Overall, the balance of evidence supports RM tornadoes as lofting more debris to higher elevations, given the lower CC values (Fig. 13) and higher TDS heights compared to QLCS EF1 tornadoes.

RM EF1 tornado translation speeds (per mean movement of WSR-88D velocity couplet centroids) are slower, on average, compared to QLCS EF1 tornadoes (~29 vs ~39 kt, respectively). The slower translation speeds result in longer durations of tornado conditions along similar pathlengths (not shown; on average ~8-min tornado duration for RM EF1 and ~5 min for QLCS EF1), which may be a partial explanation for the greater TDS depths. Regarding peak tornado wind speeds and resultant damage potential, the sum of V_{rot} and translation speed is larger for QLCS EF1 events (~7 kt larger in the mean, based on ~10-kt faster translation and ~3-kt weaker V_{rot}). This suggests somewhat greater damage potential with fast-moving QLCS tornadoes, despite a relatively weak vortex. Damage with a fast-moving (>50 kt), modest intensity vortex (V_{rot} 30–40 kt) could produce winds consistent with EF1 damage indicators but skewed to the right half of the vortex.

The combination of weaker V_{rot} and broader velocity couplets sampled slightly closer to the ground (in aggregate)

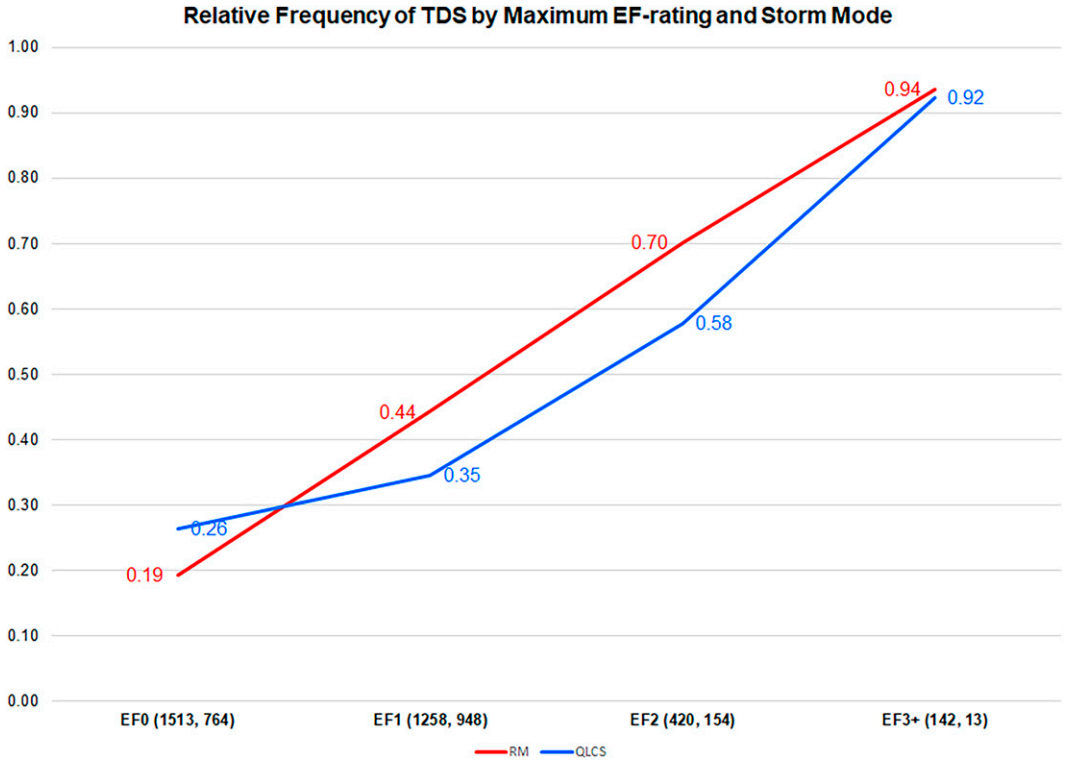

FIG. 11. Relative frequency of TDS occurrence by maximum EF-scale damage rating for RM and QLCS tornadoes (sample sizes in parentheses, respectively) from 2012 to 2021.

suggests the possibility that QLCS tornado damage might be rated EF1 too frequently. However, it is unknown to what extent EF1 damage with QLCSs is misclassified as tornadic, nor is the best way known to classify strongly asymmetric damage (skewed almost entirely to the right side of a vortex) associated with relatively weak/fast moving vortices within a QLCS.

Evidence of potentially misclassified damage is provided by a comparison of EF1 RM and QLCS tornadoes that occurred close to the radar sites (<3000 ft ARL), separated by those that occurred during the day (1500–2259 UTC) versus those that occurred overnight (0400–1159 UTC). Per Table 2, RM EF1 tornadoes produced TDSs at rates of 67% and 69% during the day versus at night, respectively. Meanwhile, QLCS EF1 tornadoes produced TDSs at rates of only 53% and 47% during the day versus at night, respectively. A lower rate of TDS occurrence during the day for RMs is somewhat expected, given the likelihood that some tornadoes can be seen without lofting enough debris to produce a TDS. In contrast, daylight QLCS EF1 tornadoes were associated with a higher relative frequency of TDSs compared to overnight QLCS tornado reports. Per a one-tailed t test assuming equal variance (Wilks 1995), there is high confidence that QLCS EF1 tornadoes produce TDSs at a lower rate overnight compared to RM EF1 tornadoes ($p = 0.0004$). On average, RM EF1 tornadoes last a few minutes longer than QLCS EF1 tornadoes, which allows more time for debris lofting. Also, the greater TDS heights occurring with RM EF1 tornadoes is indirect evidence of deeper, stronger updrafts with RM versus QLCS tornadoes. Thus, QLCS tornadoes (on average) require better WSR-88D sampling (closer to the radar site) to observe TDSs. Still, the possibility remains that some of the reported EF1 damage is misclassified as tornadic, especially with overnight QLCS tornadoes, and based on the consistently lower rate of occurrence of TDSs, even very close to the radar site (Table 1).

Weak tornadoes (i.e., F/EF0 and F/EF1) produced by both QLCSs and RMs account for ~83% of the total grid-hour tornado events in this study but are responsible for <1% of deaths and 3%–7% of injuries caused by all of the grid-hour tornado events, respectively. By comparison, EF2+ tornadoes account for ~15% of grid-hour events, but are responsible for ~93%–96% of the deaths and injuries. Like the differences noted in the radar signatures between the QLCS and RM EF2 tornadoes, injuries and damage are greater with RM EF2+ tornadoes compared to QLCS EF2+ tornadoes by a factor of 5–10, in general agreement with the earlier work by Brotzge et al. (2013). Thus, while weak (EF0) tornadoes produced by RMs and QLCSs are largely indistinguishable from one another in WSR-88D data, RM EF2+ tornadoes are typically longer lived and more dangerous than QLCS EF2+ tornadoes.

If there are measurable differences in the threat posed by QLCS tornadoes compared to RM tornadoes, then should all tornadoes be treated equally in forecasts and warnings? Current NWS directives (NWS 2022) do not specify tornado type

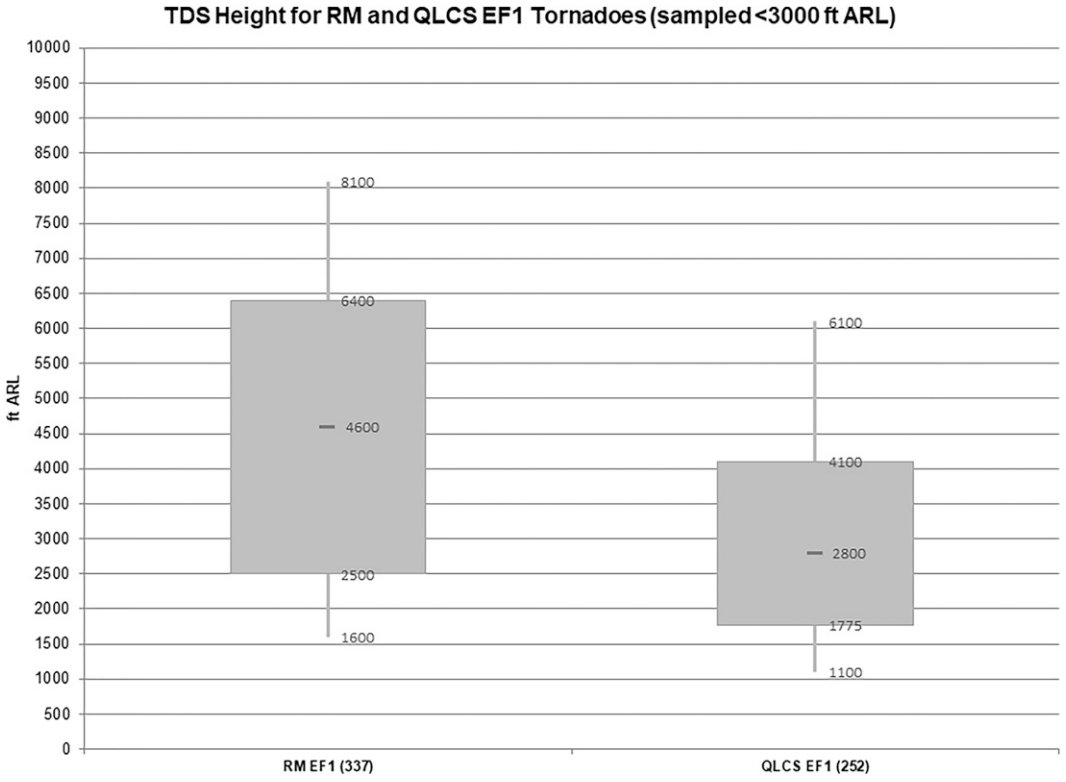

FIG. 12. Maximum height (ft ARL) of TDS signatures associated with RM and QLCS EF1 tornadoes, with minimum sampling height < 3000 ft. ARL. See section 2 for TDS criteria.

nor intensity in warning-verification metrics, so a brief EF0 (or EF-unknown) tornado counts the same as a violent (EF4–5) tornado. The lack of specificity in tornado reports, and verification efforts based on said reports, including their damage-based intensity, can lead to unintended and unexpected problems for operational meteorologists that include changes in forecast/warning procedures based almost solely on tornado-reporting practices. For example, should the increasing number of QLCS tornado reports lead to a corresponding increase in tornado watches for QLCSs? Also, the ability to justify EF2 ratings with trees alone (Wind Science and Engineering Center 2006; Edwards et al. 2021) likewise results in an increase in the number of QLCS tornadoes rated EF2 (primarily in wooded areas east of the Great Plains), which has historically been the threshold for "significant" tornadoes (Hales 1988). A relatively recent example of such extreme reporting increases can be seen in the 15 December 2021 QLCS tornado outbreak from eastern Nebraska to the upper Mississippi Valley, with 22 maximum grid-hour tornadoes rated EF2, 30 rated EF1, and only 10 tornadoes rated EF0 or EF-unknown. These tornadoes were embedded within a squall line that produced a derecho (Corfidi et al. 2016), with many measured straight-line surface wind gusts into the EF1 range. Similarly, there were 24 grid-hour tornado events (all rated EF0–1) embedded within the high-end derecho across Iowa and northern Illinois on 10 August 2020—this convective system was the most damaging severe thunderstorm event in U.S. history (causing an estimated $11 billion in damage) with straight-line wind swaths of 100 to more than 120 mph (NCEI 2022). In the 10 August 2020 event, the majority of the damage and injuries/fatalities was the result of the damaging wind swaths, and the QLCS tornadoes were of secondary importance.

TABLE 1. Relative frequency of TDS occurrence with RM and QLCS EF1 tornadoes by sampling height ARL (sample sizes in parentheses).

Sampling height	RM TDS relative frequency EF1	QLCS TDS relative frequency EF1
<3000 ft ARL	0.64 (524)	0.51 (495)
<2000 ft ARL	0.73 (300)	0.61 (311)
<1000 ft ARL	0.76 (95)	0.69 (121)

5. Summary

Overall, QLCS tornado reports have increased in the past 14 years while the number of reported RM tornadoes has decreased across the contiguous United States. The cause behind the decrease in RM tornadoes is not known with confidence but may be related a relative paucity of larger tornado outbreaks since 2013 or an eastward shift in tornado-favorable environments from the Great Plains toward the Mississippi Valley. The increase in the number of QLCS tornado reports has occurred during a period with improvements in WSR-88D velocity data resolution and implementation of scan strategies that increased

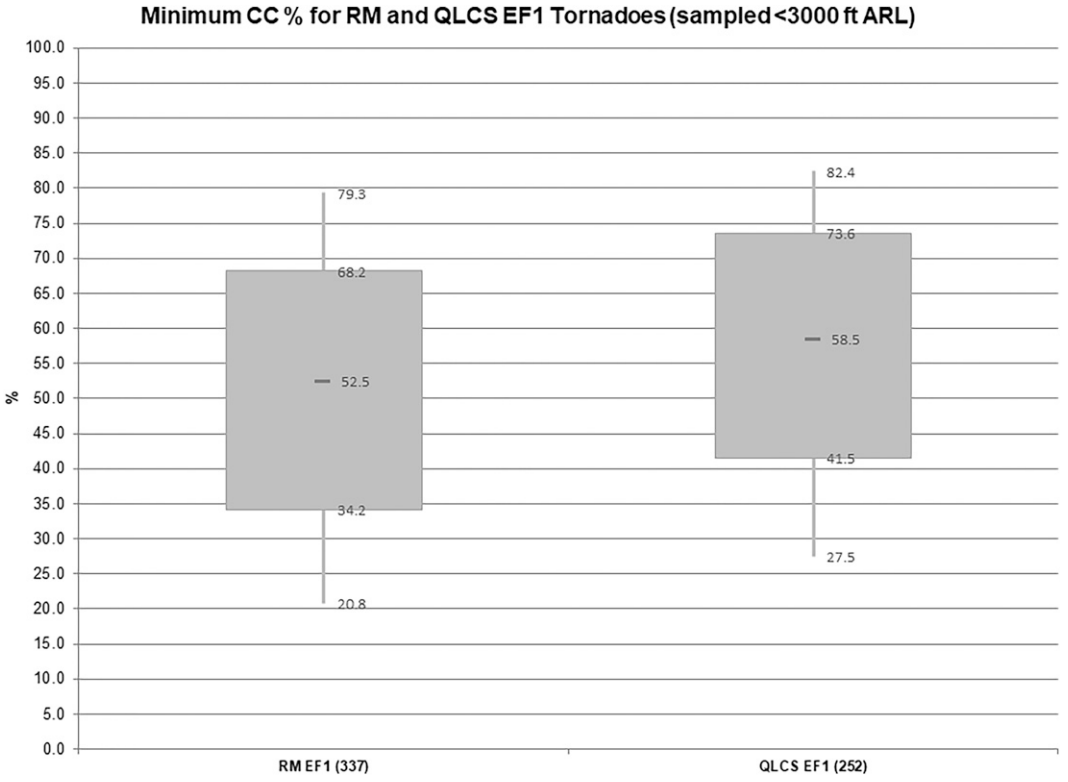

FIG. 13. Minimum cross-polar CC (%) in the lowest-elevation scan during the lifespan of each TDS with RM and QLCS EF1 tornadoes (minimum sampling height < 3000 ft ARL).

the number of radar scans closest to the ground. Emphasis on short-term forecasts of QLCS tornado potential may have also contributed to increases in both tornado warnings and tornado reports with QLCSs.

The increase in QLCS tornado reports is not without question, however. Unusual anomalies remain in the reporting of QLCS tornadoes, with a maximum frequency of occurrence for EF1-rated QLCS tornadoes, while EF0-rated tornadoes are most common with RMs. Sampling of the radar velocity couplets associated with the tornado reports, via the WSR-88D network across the CONUS, suggests that QLCS tornadoes are associated with weaker V_{rot} and broader velocity couplets, despite being sampled a little closer to the ground (closer to the radar site) compared to RM tornadoes. One could argue that QLCS tornadoes are inherently smaller (narrower) than RM tornadoes, which would affect the ability of the WSR-88D to resolve the related velocity couplets and V_{rot}, though Fig. 5 clearly shows little difference in observed tornado damage path widths between RM and QLCS tornadoes. A lower percentage of QLCS tornadoes produce TDSs for the peak damage ratings of EF1–2 ratings compared to RM tornadoes, despite the tendency for QLCS tornadoes to occur farther east than RM tornadoes in areas with more numerous and consistent potential damage indicators and lofted debris (e.g., trees and structures). These findings suggest the following:

1) Closer radar sampling (well below 3000 ft ARL) is necessary to identify relatively shallow TDSs with QLCS tornadoes, and a small fraction of QLCS wind damage reports might be misclassified as tornadic (when a TDS is not observed).
2) EF0 QLCS tornadoes may be underreported, and EF1–2 QLCS tornado ratings could be somewhat inflated, similar to the discussion by Edwards et al. (2021) regarding changes in tornado reporting following adoption of the EF scale in 2007. Conversely, a lack of damage indicators may tend to reduce the number RM tornadoes rated EF1–2 in the more open areas of the Great Plains.
3) EF1–2 damage is relatively easier to achieve on the right side of a modestly strong, fast-moving QLCS mesovortex/tornado.

TABLE 2. Relative frequency of TDS occurrence with RM and QLCS EF1 tornadoes, for those occurring during typical daylight hours (1500–2259 UTC) and during the overnight hours (0400–1159 UTC). Cases are limited to those sampled at <3000 ft ARL; sample sizes are given in parentheses.

	RM TDS relative frequency EF1	QLCS TDS relative frequency EF1
Daylight (1500–2259 UTC)	0.67 (223)	0.53 (165)
Overnight (0400–1159 UTC)	0.69 (72)	0.47 (170)

When the probability of any tornado is relatively low (e.g., weak WSR-88D signatures) and the expectation is for (at worst) relatively weak, short-lived tornadoes that are typical of the lower margins of buoyancy in high-shear, low-CAPE (HSLC; Sherburn and Parker 2014) environments, is there an opportunity to treat such situations differently than the higher-end tornado scenarios? Most tornadoes are rated F/EF0 (Smith et al. 2012), with estimated peak wind speeds of 65–85 mph (Edwards et al. 2013), and such tornadoes pose a threat to life and property that is similar to typical severe thunderstorm events with peak straight-line winds in the same speed range. Tornado warning performance is worst for the weakest and typically shortest-lived tornadoes (e.g., Brotzge et al. 2013; Gibbs 2016, 2021; Anderson-Frey et al. 2016, 2019; Anderson-Frey and Brooks 2019, 2021; Bentley et al. 2021). Moreover, the tendency to receive and respond to tornado warnings is already reduced during the early morning hours (Krocak et al. 2021), which is the time when QLCS tornadoes are more common than RM tornadoes (Trapp et al. 2005; Ashley et al. 2019). The combination of these factors brings into question the necessity for substantially different actions in response to low-end tornado threats, compared to typical severe thunderstorms with damaging winds. A counterargument, though, can be made in response to increased vulnerability of manufactured housing to even "weak" tornadoes, since this housing vulnerability coincides with areas where nocturnal QLCS tornadoes are common across the Southeast (Ashley 2007; Ashley et al. 2008; Ashley and Strader 2016; Ashley et al. 2019; Strader et al. 2022).

The differences in QLCS and RM tornadoes is not merely an exercise in semantics. There is potentially an opportunity to reduce the number of tornado warnings for relatively weak, low-impact tornadoes with most QLCSs. Likewise, this could reduce unnecessary fear in public response to relatively short-lived and weak QLCS tornadoes that are unlikely to produce damage appreciably different than straight-line winds often produced by severe QLCSs. Moreover, reducing tornado warnings, or modifying warning and forecast verification to reflect convective mode and tornado intensity, could have the added benefit of reducing pressure for increased tornado probabilities in QLCS scenarios with convective outlooks and watches. The primary mission of the NWS is the protection of life, which can be bolstered by some reduction in tornado warnings for weak tornadoes with QLCSs, potentially increasing the credibility (and subsequent effective public response) of tornado warnings (and tornado watches) in more substantial tornado scenarios.

Acknowledgments. The author thanks Bryan Smith and Andy Dean (SPC) for their continued assistance in assembling and updating the tornado and convective mode sample that forms the basis of this work. Andrew Lyons (SPC) kindly produced the graphics for Fig. 4. The efforts of Israel Jirak (SPC) are also appreciated in helping refine the presentation and clarity of this work. Matthew Bunkers, Victor Gensini, Kevin Skow, and an anonymous reviewer suggested multiple improvements to the original submission.

Data availability statement. The raw convective mode data are available, in either Excel or .csv format, upon request.

REFERENCES

Anderson-Frey, A. K., and H. Brooks, 2019: Tornado fatalities: An environmental perspective. *Wea. Forecasting*, **34**, 1999–2015, https://doi.org/10.1175/WAF-D-19-0119.1.

——, and ——, 2021: Compared to what? Establishing environmental baselines for tornado warning skill. *Bull. Amer. Meteor. Soc.*, **102**, E738–E747, https://doi.org/10.1175/BAMS-D-19-0310.1.

——, Y. P. Richardson, A. R. Dean, R. L. Thompson, and B. T. Smith, 2016: Investigation of near-storm environments for tornado events and warnings. *Wea. Forecasting*, **31**, 1771–1790, https://doi.org/10.1175/WAF-D-16-0046.1.

——, ——, ——, ——, and ——, 2019: Characteristics of tornado events and warnings in the southeastern United States. *Wea. Forecastiing*, **34**, 1017–1034, https://doi.org/10.1175/WAF-D-18-0211.1.

Ashley, W. S., 2007: Spatial and temporal analysis of tornado fatalities in the United States: 1880–2005. *Wea. Forecasting*, **22**, 1214–1228, https://doi.org/10.1175/2007WAF2007004.1.

——, A. J. Krmenec, and R. Schwantes, 2008: Vulnerability due to nocturnal tornadoes. *Wea. Forecasting*, **23**, 795–807, https://doi.org/10.1175/2008WAF2222132.1.

——, and S. M. Strader, 2016: Recipe for disaster: How the dynamic ingredients of risk and exposure are changing the tornado disaster landscape. *Bull. Amer. Meteor. Soc.*, **97**, 767–786, https://doi.org/10.1175/BAMS-D-15-00150.1.

——, A. M. Harberlie, and J. Strohm, 2019: A climatology of quasi-linear convective systems and their hazards in the United States. *Wea. Forecasting*, **34**, 1605–1631, https://doi.org/10.1175/WAF-D-19-0014.1.

Atkins, N. T., and M. St. Laurent, 2009a: Bow echo mesovortices. Part I: Processes that influence their damaging potential. *Mon. Wea. Rev.*, **137**, 1497–1513, https://doi.org/10.1175/2008MWR2649.1.

——, and ——, 2009b: Bow echo mesovortices. Part II: Their genesis. *Mon. Wea. Rev.*, **137**, 1514–1532, https://doi.org/10.1175/2008MWR2650.1.

Bentley, E. S., R. L. Thompson, B. R. Bowers, J. G. Gibbs, and S. E. Nelson, 2021: An analysis of 2016–18 tornadoes and National Weather Service tornado warnings across the contiguous United States. *Wea. Forecasting*, **36**, 1909–1924, https://doi.org/10.1175/WAF-D-20-0241.1.

Bothwell, P. D., J. A. Hart, and R. L. Thompson, 2002: An integrated three-dimensional objective analysis scheme in use at the Storm Prediction Center. *21st Conf. on Severe Local Storms/19th Conf. on Weather Analysis and Forecasting/15th Conf. on Numerical Weather Prediction*, San Antonio, TX, Amer. Meteor. Soc., JP3.1, https://ams.confex.com/ams/SLS_WAF_NWP/techprogram/paper_47482.htm.

Brooks, H. E., and Coauthors, 2019: A century of progress in severe convective storm research and forecasting. *A Century of Progress in Atmospheric and Related Sciences: Celebrating the American Meteorological Society Centennial*, *Meteor. Monogr.*, No. 59, Amer. Meteor. Soc., https://doi.org/10.1175/AMSMONOGRAPHS-D-18-0026.1.

Brotzge, J. A., S. E. Nelson, R. L. Thompson, and B. T. Smith, 2013: Tornado probability of detection and lead time as a function of convective mode and environmental parameters. *Wea. Forecasting*, **28**, 1261–1276, https://doi.org/10.1175/WAF-D-12-00119.1.

Brown, R. A., B. A. Flickinger, E. Forren, D. M. Schultz, D. Sirmans, P. L. Spencer, V. T. Wood, and C. L. Ziegler, 2005: Improved detection of severe storms using experimental fine-resolution

WSR-88D measurements. *Wea. Forecasting*, **20**, 3–14, https://doi.org/10.1175/WAF-832.1.

Chrisman, J., 2014: Multiple elevation scan option for SAILS (MESO-SAILS). NOAA Rep., 27 pp., https://www.roc.noaa.gov/wsr88d/PublicDocs/NewTechnology/MESO-SAILS_Description_Briefing_Jan_2014.pdf.

Corfidi, S. F., M. C. Coniglio, A. E. Cohen, and C. M. Mead, 2016: A proposed revision to the definition of "derecho." *Bull. Amer. Meteor. Soc.*, **97**, 935–949, https://doi.org/10.1175/BAMS-D-14-00254.1.

Edwards, R., J. G. LaDue, J. T. Ferree, K. Scharfenberg, C. Maier, and W. L. Colbourne, 2013: Tornado intensity estimation: Past, present, and future. *Bull. Amer. Meteor. Soc.*, **22**, 641–653, https://doi.org/10.1175/BAMS-D-11-00006.1.

——, H. E. Brooks, and H. Cohn, 2021: Changes in tornado climatology accompanying the enhanced Fujita scale. *J. Appl. Meteor. Climatol.*, **60**, 1465–1482, https://doi.org/10.1175/JAMC-D-21-0058.1.

Flournoy, M. D., and M. C. Coniglio, 2019: Origins of vorticity in a simulated tornadic mesovortex observed during PECAN on 6 July 2015. *Mon. Wea. Rev.*, **147**, 107–134, https://doi.org/10.1175/MWR-D-18-0221.1.

Gallus, W. A., Jr., N. A. Snook, and E. V. Johnson, 2008: Spring and summer severe weather reports over the Midwest as a function of convective mode: A preliminary study. *Wea. Forecasting*, **23**, 101–113, https://doi.org/10.1175/2007WAF2006120.1.

Gensini, V. A., and H. E. Brooks, 2018: Spatial trends in United States tornado frequency. *npj Climate Atmos. Sci.*, **1**, 38, https://doi.org/10.1038/s41612-018-0048-2.

Gibbs, J. G., 2016: A skill assessment of techniques for real-time diagnosis and short-term prediction of tornado intensity using the WSR-88D. *J. Oper. Meteor.*, **4**, 170–181, https://doi.org/10.15191/nwajom.2016.0413.

——, 2021: Evaluating precursor signals for QLCS tornado and higher impact straight-line wind events. *J. Oper. Meteor.*, **9**, 62–75, https://doi.org/10.15191/nwajom.2021.0905.

Hales, J. E., Jr., 1988: Improving the watch/warning program through use of significant event data. Preprints, *15th Conf. on Severe Local Storms*, Baltimore, MD, Amer. Meteor. Soc., 165–168.

Krocak, M. J., J. N. Allan, J. T. Ripberger, C. L. Silva, and H. C. Jenkins-Smith, 2021: An analysis of tornado warning reception and response across time: Leveraging respondents' confidence and a nocturnal tornado climatology. *Wea. Forecasting*, **36**, 1649–1660, https://doi.org/10.1175/WAF-D-20-0207.1.

Lyons, A. D., B. T. Smith, R. L. Thompson, and A. R. Dean, 2022: Convective mode classification and climatology of tornado events in the contiguous United States 2000–2020. *30th Conf. on Severe Local Storms*, Santa Fe, NM, Amer. Meteor. Soc., P28, https://ams.confex.com/ams/30SLS/meetingapp.cgi/Paper/407288.

Lyza, A. W., R. Castro, E. Lenning, M. T. Friedlein, B. S. Borchardt, A. W. Clayton, and K. R. Knupp, 2019: A multi-platform reanalysis of the Kankakee Valley tornado cluster on 30 June 2014. *Electron. J. Severe Storms Meteor.*, **14** (3), https://ejssm.com/ojs/index.php/site/article/view/73.

McDonald, J. M., and C. C. Weiss, 2021: Cold pool characteristics of tornadic quasi-linear convective systems and other convective modes observed during VORTEX-SE. *Mon. Wea. Rev.*, **149**, 821–840, https://doi.org/10.1175/MWR-D-20-0226.1.

NCEI, 2022: U.S. billion-dollar weather and climate disasters, 1980–present (NCEI Accession 0209268). NCEI, accessed 12 December 2022, https://doi.org/10.25921/stkw-7w73.

NWS, 2022: NWS Directives System. NOAA, https://www.nws.noaa.gov/directives/010/010.php.

Parker, M. D., B. S. Borchardt, R. L. Miller, and C. L. Ziegler, 2020: Simulated evolution and severe wind production by the 25–26 June 2015 nocturnal MCS from PECAN. *Mon. Wea. Rev.*, **148**, 183–209, https://doi.org/10.1175/MWR-D-19-0072.1.

Ryzhkov, A. V., T. J. Schuur, D. W. Burgess, and D. S. Zrnić, 2005: Polarimetric tornado detection. *J. Appl. Meteor.*, **44**, 557–570, https://doi.org/10.1175/JAM2235.1.

Schaumann, J. S., and R. W. Przybylinski, 2012: Operational application of 0–3 km bulk shear vectors in assessing quasi-linear convective system mesovortex and tornado potential. *26th Conf. on Severe Local Storms*, Nashville, TN, Amer. Meteor. Soc., 142, https://ams.confex.com/ams/26SLS/webprogram/Paper212008.html.

Schenkman, A. D., and M. Xue, 2016: Bow-echo mesovortices: A review. *Atmos. Res.*, **170**, 1–13, https://doi.org/10.1016/j.atmosres.2015.11.003.

Schultz, C. J., and Coauthors, 2012a: Dual-polarization tornadic debris signatures Part I: Examples and utility in an operational setting. *Electron. J. Oper. Meteor.*, **13** (9), 120–137, http://nwafiles.nwas.org/ej/pdf/2012-EJ9.pdf.

——, and Coauthors, 2012b: Dual-polarization tornadic debris signatures Part II: Comparisons and caveats. *Electron. J. Oper. Meteor.*, **13** (10), 138–150, http://nwafiles.nwas.org/ej/pdf/2012-EJ10.pdf.

Sherburn, K. D., and M. D. Parker, 2014: Climatology and ingredients of significant severe convection in high-shear, low-CAPE environments. *Wea. Forecasting*, **29**, 854–877, https://doi.org/10.1175/WAF-D-13-00041.1.

Skow, K. D., and C. Cogil, 2017: A high-resolution aerial survey and radar analysis of quasi-linear convective system surface vortex damage paths from 31 August 2014. *Wea. Forecasting*, **32**, 441–467, https://doi.org/10.1175/WAF-D-16-0136.1.

Smith, B. T., R. L. Thompson, J. S. Grams, C. Broyles, and H. E. Brooks, 2012: Convective modes for significant severe thunderstorms in the contiguous United States. Part I: Storm classification and climatology. *Wea. Forecasting*, **27**, 1114–1135, https://doi.org/10.1175/WAF-D-11-00115.1.

——, ——, A. R. Dean, and P. T. Marsh, 2015: Diagnosing the conditional probability of tornado damage rating using environmental and radar attributes. *Wea. Forecasting*, **30**, 914–932, https://doi.org/10.1175/WAF-D-14-00122.1.

Strader, S. M., W. S. Ashley, A. M. Haberlie, and K. Kaminski, 2022: Revisiting U.S. nocturnal tornado vulnerability and its influence on tornado impacts. *Wea. Climate Soc.*, **14**, 1147–1163, https://doi.org/10.1175/WCAS-D-22-0020.1.

Thompson, R. L., B. T. Smith, J. S. Grams, and C. Broyles, 2012: Convective modes for significant severe thunderstorms in the contiguous United States. Part II: Supercell and QLCS tornado environments. *Wea. Forecasting*, **27**, 1136–1154, https://doi.org/10.1175/WAF-D-11-00116.1.

——, and Coauthors, 2017: Tornado damage rating probabilities derived from WSR-88D data. *Wea. Forecasting*, **32**, 1509–1528, https://doi.org/10.1175/WAF-D-17-0004.1.

Torres, S., and C. Curtis, 2007: Initial implementation of super-resolution data on the NEXRAD network. *23rd Int. Conf. on Interactive Information and Processing Systems for Meteorology, Oceanography, and Hydrology*, San Antonio, TX, Amer. Meteor. Soc., 5B.10, https://ams.confex.com/ams/87ANNUAL/techprogram/paper_116240.htm.

Trapp, R. J., and M. L. Weisman, 2003: Low-level mesovortices within squall lines and bow echoes. Part II: Their genesis and implications. *Mon. Wea. Rev.*, **131**, 2804–2823, https://doi.org/10.1175/1520-0493(2003)131<2804:LMWSLA>2.0.CO;2.

——, S. A. Tessendorf, E. S. Godfrey, and H. E. Brooks, 2005: Tornadoes from squall lines and bow echoes. Part I: Climatological distribution. *Wea. Forecasting*, **20**, 23–34, https://doi.org/10.1175/WAF-835.1.

Van Den Broeke, M. S., and S. T. Jauernic, 2014: Spatial and temporal characteristics of polarimetric tornadic debris signatures. *J. Appl. Meteor. Climatol.*, **53**, 2217–2231, https://doi.org/10.1175/JAMC-D-14-0094.1.

Weisman, M. L., and R. J. Trapp, 2003: Low-level mesovortices within squall lines and bow echoes. Part I: Overview and dependence on environmental shear. *Mon. Wea. Rev.*, **131**, 2779–2803, https://doi.org/10.1175/1520-0493(2003)131<2779:LMWSLA>2.0.CO;2.

Wilks, D. S., 1995: *Statistical Methods in the Atmospheric Sciences: An Introduction*. Academic Press, 467 pp.

Wind Science and Engineering Center, 2006: A recommendation for an enhanced Fujita scale (EF-scale). Texas Tech University Wind Science and Engineering Center Rep., 95 pp., https://www.spc.noaa.gov/faq/tornado/ef-ttu.pdf.